

Effects of Monovalent Anions of the Hofmeister Series on DPPC Lipid Bilayers Part II: Modeling the Perpendicular and Lateral Equation-of-State

E. Leontidis,* A. Aroti,* L. Belloni,[†] M. Dubois,[†] and T. Zemb[†]

*Department of Chemistry, University of Cyprus, Nicosia, Cyprus; and [†]CEA/Laboratoire Interdisciplinaire sur l'Organisation Nanométrique et Supramoléculaire at Département de Recherche sur l'État Condensé, les Atomes, et les Molécules Service de Chimie Moléculaire at Commissariat à l'Energie Atomique, Saclay, F91191 Gif sur Yvette, France

ABSTRACT The effects of Hofmeister anions on the perpendicular and lateral equation-of-state (EOS) of the dipalmitoylphosphatidylcholine lamellar phase discussed in the companion article are here examined using appropriate free energy models for the intra- and interbilayer interactions. Minimizing the free energy with respect to the two basic geometrical parameters of the lamellar phase, which are the interbilayer water thickness, d_w , and the lipid headgroup area, a_L , provides the perpendicular (osmotic pressure balance) and lateral EOS. Standard models were used for the hydration, undulation, and Van der Waals attractive force between the bilayers in the presence of electrolytes whereas two alternative treatments of electrostatic interactions were used to obtain “binding” or “partitioning” constants of anions to the lipid bilayers both in the absence and in the presence of sodium binding. The computed binding constants depend on anion type and follow the Hofmeister series, but were found to increase with electrolyte concentration, implying that the local binding approximation cannot fit bilayer repulsion data. The partitioning model was also found inadequate at high electrolyte concentrations. The fitting attempts revealed two additional features worthy of future investigation. First, at maximum swelling in the presence of electrolytes the osmotic pressure of the bilayer system cannot be set equal to zero. Second, at high salt concentrations an additional repulsion appears to come into effect in the presence of strongly adsorbing anions such as I^- or SCN^- . Both these phenomena may reflect an inconsistent treatment of the ion-surface interactions, which have an impact on the osmotic pressure. Alternatively, they may arise from bulk solution nonidealities that cannot be handled by the classical Poisson-Boltzmann formalism. The inability of current models to explain the “lateral” EOS by fitting the area per lipid headgroup as a function of salt type and concentration shows that current understanding of phospholipid-ion interactions is still very incomplete.

INTRODUCTION

In the companion article in this series (1) we described osmotic stress experiments on dipalmitoylphosphatidylcholine (DPPC) bilayers (above the chain melting temperature) in the presence of a range of concentrations of various sodium salts. The objective was to use DPPC bilayers in water (L_α phase in equilibrium with excess water) as a model system for the investigation of the mechanism of action of monovalent anions belonging to the Hofmeister series (2–4). Here we undertake a quantitative analysis, by fitting both the “perpendicular” (osmotic pressure versus bilayer distance, $\log \Pi$ vs. d_w) and the “lateral” (area per DPPC headgroup, a_L , as a function of salt type and concentration) equation-of-state (EOS) data to interaction models that take into account the effects of salts.

Osmotic stress experiments (5–7) are currently the principal method to measure the osmotic pressure EOS of phospholipid bilayers (5–15). Much less work has been done on the measurement of the lateral compressibility of bilayers or the lateral EOS (16). Correspondingly, theoretical attention has mostly focused on the perpendicular EOS (17–24) and seldom on the lateral EOS (24–27). The area per headgroup is however obtained from a combination of complementary

measurements, and the lateral EOS provides an additional opportunity (and a challenge) to test models for specific ion effects. A successful model should in fact be capable of reproducing both the perpendicular and lateral EOS of lipid bilayers. The simplest way to simultaneously work on both EOS is to consider a free energy expression for the bilayer system, which contains both in-plane and out-of-plane components, and also, inevitably, cross-terms. Minimization of the free energy with respect to the two principal geometric parameters, d_w and a_L , eventually provides the two EOS. In this approach it is necessary to have available a complete free energy expression for a system of interacting bilayers, which must contain all terms that depend on d_w and a_L .

The interaction between bilayers is supposed to be the sum of three to four “independent” forces, some of them empirical in nature, all of which introduce adjustable parameters. In this work we use the four standard interactions that appear in almost all recent related investigations (8–19,23), namely the Van der Waals attractive force, the hydration force, the fluctuation force and the electrostatic force. The effect of electrolytes on the Hamaker constant and bending rigidity of DPPC bilayers is here treated according to literature information, which suggests that the Hamaker constant could be reduced by 50% or more (23,28,29) and the bending rigidity should also decrease (30) in specific ways in the presence of electrolytes. In addition, we make the usual

Submitted March 19, 2007, and accepted for publication April 23, 2007.

Address reprint requests to E. Leontidis, E-mail: psleon@ucy.ac.cy.

Editor: Antoinette Killian.

© 2007 by the Biophysical Society

0006-3495/07/09/1591/17 \$2.00

doi: 10.1529/biophysj.107.109264

assumption (8,17,19,23,31,32) that the preferential association of one or both ions of the electrolyte with the neutral phospholipid headgroups generates charged layers at the lipid-water interfaces, which create an additional electrostatic repulsion over what is observed in the absence of electrolytes. There are several alternative ways to model this ion-lipid association however, as we recently discussed (33). In this attempt we use both the local binding approach, and also a “penetration” model, which assumes that anions penetrate uniformly the lipid headgroup layer, although alternative models have been proposed (22,24). These two models were found to be nonequivalent in the case of DPPC monolayers at the air-water interface ((34); E. Leontidis, L. Belloni, and A. Aroti, unpublished data). The penetration model is not a new idea, since it has been used in the past to model the surface pressure of insoluble monolayers at the air-water interface (35) and also the surfaces of soft colloidal particles like micelles (36). However, it is used here in the spirit of the more general picture of an “active interface”, according to which ions may preferentially partition inside a lipid layer provided that this layer is disordered enough and that the system gains free energy from the liberation of water molecules of the first hydration shells (33,34,37).

The lateral EOS is obtained from the minimization of the free energy with respect to the headgroup area. There is no established way to partition the intralayer free energy into “independent” components. The in-plane terms are assumed here to be: a), the lipid-water “contact” free energy, modeled as an interfacial tension term; b), the contribution of the conformational entropy of the lipid tails; and c), the non-electrostatic repulsive energy between headgroups (24–27, 33,38–41). Cross-terms, describing interactions between two bilayer sheets, also contribute to the lateral EOS. These are the electrostatic energy and the Van der Waals interaction, since both depend on the headgroup area of the lipids.

We believe that the use of two alternative electrostatic models for the ion-lipid association, the examination of the effect of both anion and sodium binding on the lipid headgroups, and—most importantly—the combined modeling of perpendicular and lateral EOS information presented in this work provide a comprehensive modeling platform to improve our understanding of specific salt effects on lipid systems. To our knowledge, an investigation of such a wide range does not exist in the relevant literature to date.

Theoretical analysis

Steps toward the derivation of the perpendicular and lateral EOS

In the companion article (1) we have described the experimental system of bilayer stacks swollen by water and immersed in a solution of polymeric chains that cannot penetrate the lipid phase. In the osmotic stress experiment it is generally assumed that the polymer solution acts as an infinite reservoir of water and ions for the bilayer phase, its osmotic

pressure remaining largely unaffected as salt is added (1,5,34). With this basic assumption we focus only on the free energy of the lipid bilayer phase. To properly formulate EOS for this phase one can start either from a partition function of the bilayer system (38,42,43) or from an empirical free energy expression (21,22,24–27). Although it is a very difficult problem to dissect the bilayer free energy into physically distinct components, an empirical break-up of the free energy is adopted by most workers in the area, and will be attempted in this work as well. We will write the free energy as a function of two principal geometric parameters, which we choose to be the interbilayer water thickness, d_w , and the area per lipid headgroup, a_L . Experimentally, d_w is obtained from the measured period of the lamellar phase, D , and the lipid volume fraction in that phase, ϕ_L (1,5–13).

$$d_w = D - b_L = D(1 - \phi_L). \quad (1)$$

The area per headgroup is also indirectly obtained from the same data through the bilayer thickness, b_L , as explained in the previous article (1):

$$a_L = \frac{2 \times M_L \times \bar{v}_L}{b_L \times N_{AV}}, \quad (2)$$

where M_L is the lipid molecular weight, N_{AV} is Avogadro's number, and \bar{v}_L is the partial specific volume of the phospholipid molecule. The free energy of the bilayer stack contains intralayer (lateral) terms, bilayer-interaction terms, and coupling or cross-terms. The electrostatic term is such a cross-term at close distances, since it may depend on both principal geometric parameters. The Van der Waals attraction is another such term, since it depends on d_w and b_L , the latter being related to the headgroup area through Eq. 2. We assume that the reference state for the calculation of free energy differences is a hypothetical lipid “crystal” containing n_L molecules at the temperature of the experiment (26, 39,40) and an infinite electrolyte solution with a monovalent salt concentration equal to C_∞ . We write the total free energy difference per mol of lipid as follows:

$$\Delta F_{\text{tot}} = \Delta F_{\text{intra}} + \Delta F_{\text{inter}} + \Delta F_{\text{cross}}, \quad (3)$$

and we assume, as a first approximation, that

$$\Delta F_{\text{intra}} = \Delta F_{L/W} + \Delta F_{\text{head-rep}} + \Delta F_{\text{conf}} \quad (4)$$

$$\Delta F_{\text{inter}} = \Delta F_{\text{hydr}} + \Delta F_{\text{und}} \quad (5)$$

$$\Delta F_{\text{cross}} = \Delta F_{\text{ele}} + \Delta F_{\text{vdw}}. \quad (6)$$

The intrabilayer free energy contains contributions from the lipid-water interfacial energy, the headgroup nonelectrostatic repulsion, and the conformational entropy of the tails. We initially assume that these depend only on a_L , which is a good approximation in the absence of salts. However, in the presence of salts these terms may depend on d_w , through the ionic adsorption taking place, as will be discussed below. The hydration and undulation forces are considered as pure interbilayer interaction terms depending only on d_w . This is a

usual assumption in the literature, but it must be pointed out that the nature of the hydration force and its effect on the undulation force are still poorly understood (5–7,10,11,44–55). Electrostatic and dispersion interactions depend on both d_w and a_L and are viewed as cross-terms. The osmotic pressure is obtained from the free energy difference via:

$$\frac{1}{a_L N_{AV}} \left(\frac{\partial \Delta F_{tot}}{\partial d_w} \right)_{a_L, T, n_L} = -\Pi_{tot}. \quad (7)$$

If the in-plane free energy terms of Eq. 4 do not depend on d_w , they do not contribute to the osmotic pressure, and Eq. 7 leads to the usual expression for the osmotic pressure, with the four terms (hydration, undulation, dispersion, electrostatics) currently used by most investigators, as mentioned before. Also starting from ΔF_{tot} and minimizing with respect to a_L at fixed d_w , T , n_L , we obtain the lateral EOS of the bilayer system, assuming that the bilayers are laterally free to adopt the optimal area per molecule:

$$\left(\frac{\partial \Delta F_{tot}}{\partial a_L} \right)_{d_w, T, n_L} = 0. \quad (8)$$

The ΔF_{inter} terms of Eq. 5, which depend only on d_w , will not contribute to the lateral EOS.

Perpendicular EOS

Based on Eqs. 3–7 we find the following expression for the applied osmotic pressure to the lipid bilayers, Π_{TOT} , as a function of the water bilayer separation, d_w :

$$\Pi_{tot} = \Pi_{hydr} + \Pi_{und} + \Pi_{vdw} + \Pi_{ele}. \quad (9)$$

At large distances between the bilayers, the equilibrium spacing (maximum swelling) is determined by the balance between the attractive Van der Waals forces and either electrostatic or specific hydration repulsive forces. Because DPPC is a zwitterionic lipid, electrostatic interactions exist only when the lipid layers are charged by ion adsorption. At separations shorter than ~ 20 Å the $\log \Pi - d_w$ curve provides valuable information about the hydration interaction, which overwhelms electrostatics in this distance range (5–7,53–55). In Eq. 9, Π_{hydr} is the so-called “hydration” repulsive force. This is usually empirically modeled (5–7,10–19,56–61) as an exponentially decaying function of the form:

$$\Pi_{hydr} = P_0 e^{-d_w/\lambda}, \quad (10)$$

where P_0 is the hydration coefficient, and λ is the hydration decay length, assumed here to be independent of d_w and a_L . Alternative expressions exist for this force (59,60), complicating the comparison of fitting parameters obtained by different investigators. Π_{und} is the undulation (Helfrich) repulsive force. The undulation force plays a role at relatively large distances between the bilayers (50,62). This osmotic pressure component can be modeled in a number of ways. We have used here primarily the standard power-law expression (14,15,60,61):

$$\Pi_{und} = \frac{3\pi^2 (k_B T)^2}{64\kappa_c} \frac{1}{d_w^3}, \quad (11)$$

where κ_c is the bending rigidity of the bilayers. For the sake of comparison we have also used an alternative expression that assumes coupling between the hydration and undulation forces (51,59,62–67):

$$\Pi_{und} = \frac{\pi k_B T}{32\lambda} \left(\frac{P_0}{\kappa_c \lambda} \right)^{1/2} e^{-d_w/2\lambda}. \quad (12)$$

Π_{vdw} is the Van der Waals attractive force, modeled here with an equation routinely used by all investigators today (8,9,14,15,23,59,60), although it is strictly valid for two interacting bilayers, whereas more complicated equations exist for bilayer stacks (29,68,69):

$$\Pi_{vdw} = -\frac{H}{6\pi} \left[\frac{1}{d_w^3} + \frac{1}{(d_w + 2b_L)^3} - \frac{2}{(d_w + b_L)^3} \right]. \quad (13)$$

Here H is the Hamaker constant, and b_L is the bilayer thickness, which is inversely proportional to the lipid head-group area, according to Eq. 2. Π_{ele} is the electrostatic contribution to the osmotic pressure. This is computed using the osmotic pressure at the midplane between two bilayers facing each other (54,55):

$$\begin{aligned} \Pi_{ele} &= \Pi_{osm,med} - \Pi_{osm,ref} = k_B T \sum_i \{C_{i,med} - C_{i,\infty}\} \\ &= k_B T \left\{ \sum_i C_{i,\infty} \left[\exp\left(-\frac{z_i q_e \varphi_{med}}{k_B T}\right) - 1 \right] \right\}. \end{aligned} \quad (14)$$

Here, $C_{i,\infty}$ is the concentration of ionic species i in the reference solution and $C_{i,med}$ and φ_{med} are the ionic concentration and the electrostatic potential at the midplane between the bilayers. Equation 14 implies that both the solution between the bilayers and the reference solution behave ideally and follow Van t' Hoff's law. Although this is a standard assumption in the literature (8,14,15,54,55), it is a point that must be remembered when discussing the results. In addition, the last equality in Eq. 14 assumes a Poisson-Boltzmann-type description for the diffuse double layer forming between two bilayers. The computation of Π_{ele} can be carried out numerically and requires the solution of the electrostatic problem between the bilayers and the calculation of the midplane potential, φ_{med} . Alternative models for the double layer will provide different values for φ_{med} , hence different Π_{ele} contributions.

Lateral EOS

The part of the free energy that depends on a_L is, according to Eqs. 4 and 6:

$$\begin{aligned} \Delta F(a_L) &= \Delta F_{intra} + \Delta F_{cross} = \Delta F_{L/W} + \Delta F_{head-rep} \\ &\quad + \Delta F_{conf} + \Delta F_{ele} + \Delta F_{vdw}. \end{aligned} \quad (15)$$

The free energy contribution (in J (mol lipid)^{−1}) arising from Van der Waals forces is simply the integral of Eq. 13 over d_w multiplied by the area per mol of lipid:

$$\Delta F_{\text{vdw}} = -\frac{HN_{\text{AV}}a_L}{12\pi} \left[\frac{1}{d_w^2} + \frac{1}{(d_w + 2b_L)^2} - \frac{2}{(d_w + b_L)^2} \right]. \quad (16)$$

The electrostatic free energy expression depends on the model assumed for the ionic adsorption at the lipid-water interface and will be discussed below. For the first three contributions we use models that were effective in the prediction of the area per surfactant molecule in lipid aggregates such as monolayers, bilayers, and micelles in the absence of electrolytes (24–27,33,38–41). We thus set:

$$\Delta F_{L/W} = \gamma N_{\text{AV}}(a_L - a_0). \quad (17)$$

Equation 17 describes the penalty for creating a lipid-water interface per mol of lipid; γ is the interfacial tension of this interface and a_0 is the “incompressible” headgroup area of a lipid molecule calculated from the cross section of a molecular model for double-chain lipids. For DPPC we will set a_0 equal to 42 Å² and γ equal to 50 mN m^{−1}, values generally acceptable for lipid-water interfaces (53,54,70–72). The nonelectrostatic (e.g., steric) repulsions between headgroups have been modeled with various empirical equations in the past (25,26,33,38–41,54,73), but there is no rigorous theory for this term. Stigter and Dill (74–76) provided a complex formalism for the evaluation of the headgroup repulsion term, but it is not clear how to generalize this treatment in the presence of salts. Mbamala et al. (27) have recently presented an interesting model for the lipid-water interface for a mixture of zwitterionic and cationic lipids, which assumes that salts change the average tilt of the lipids in a quasicontinuous way. The model assumed in their work is difficult to generalize in the case of charging by adsorption treated here. In this investigation we adopted a hard-disk-like formalism used by several authors in the past (26,39–41), according to which:

$$\Delta F_{\text{head-rep}} = -\mathcal{RT} \ln \left(1 - \frac{a_0}{a_L} \right). \quad (18)$$

A more elaborate equation based on the integration of the surface pressure equation for hard disks was presented by Yuet et al. (25). It has been tried in test calculations without providing improved results. An additional possible equation for the headgroup repulsion can be found in the literature (33) and has also been examined in this work:

$$\Delta F_{\text{head-rep}} = \frac{B(\mu_w)}{a_L - a_0}. \quad (19)$$

$B(\mu_w)$ is a parameter, which depends on the chemical potential of water, and can be considered roughly constant at a fixed salt concentration. The configurational free energy of the lipid chains in bilayers has been calculated using statistical mechanical theories by a number of investigators (26,38,77–79). The work by Fattal et al. (26) explicitly pro-

vided calculations for DPPC-like lipids with two C₁₆ tails, albeit at 300 K. It is expected that this free energy term may not change too much with temperature, apart from the linear “kT” scaling (A. Ben-Shaul, personal communication, 2007). Because we could not find any results for 50°C in the literature, we decided to use the results of Fattal et al. (26). We have, therefore, fitted the DPPC bilayer curves provided by these authors as a function of area per molecule with the following expression, valid for 50°C:

$$\Delta F_{\text{conf}}(\text{kJ mol}^{-1}) = -55.88 + 2957.0 \exp(-10.07a_L) + 2.981a_L, \quad (20)$$

where a_L is in nanometers. It appears that the literature contains almost no information about the way that the expressions of Eqs. 17–20 are modified in the presence of adsorbing electrolytes. It is reasonable to assume that the presence of ions at the lipid-water interface provides further screening of hydrophobic interactions. This effect can be modeled by replacing a_0 in Eq. 17 with $a_0 + x_b \Delta a_i$, where x_b is the fraction of lipid molecules with “bound ions” and Δa_i is an ionic cross section calculated from the (hydrated) ionic volume (for I[−] and SCN[−] this is close to 0.2 nm²) (80–82). It is not obvious that a similar modification would be applicable to Eqs. 18 or 19 in the presence of salts. We assume that Eq. 20 will not be modified in the presence of salts, although if the headgroup tilt is strongly affected through ion adsorption, or if anion penetration in the bilayer is too strong, the conformational statistics of the hydrocarbon tails should be affected.

Electrical free energy and ion adsorption models

In this work we have used quite high electrolyte concentrations. If the bilayer lipids were charged, the electrostatic interactions would have been screened at high salt, and the precise treatment of electrostatics would not matter much. However, the bilayers acquire charge through ionic adsorption, so it is not clear at which salt concentration screening starts to dominate the enhanced charging by adsorption. This being the case, the proper treatment of electrostatics is crucial in our systems. We will assume that the mean-field Poisson-Boltzmann equation suffices to describe the diffuse part of the double layer created between two lipid bilayers. We will ignore the coupling between water polarization and electrostatics (32,53,83–85), local dielectric saturation effects (86–89), and ion-ion interactions (90–91) and will concentrate only on the mechanism of ion adsorption at the lipid-water interface. Two alternative models are used for this adsorption process.

Model of local binding

Ion binding to the headgroups of the lipid molecules DPPC (Fig. 1 *a*) has often been modeled as a chemical reaction at the surface between an ion (here a monovalent anion) A[−]

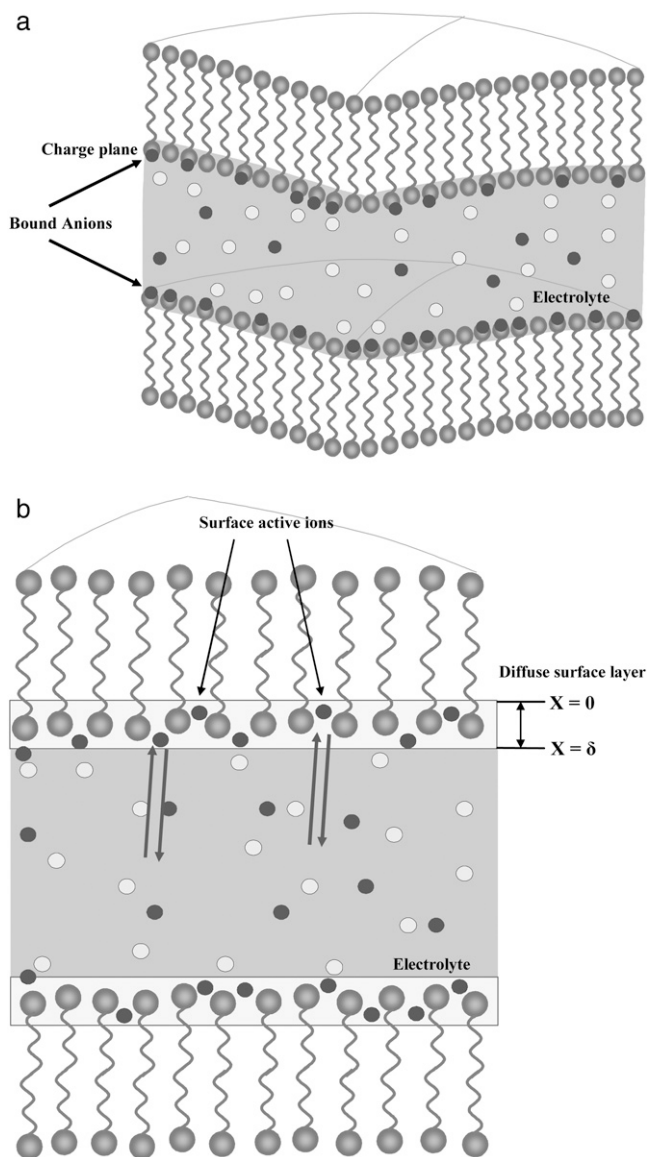


FIGURE 1 (a) Model of local binding. Binding of the anions on the headgroups of the DPPC molecules at a bilayer. (●) Anions; (○) cations. (b) Model of partitioning into a diffuse lipid layer. Partitioning of the anions between the diffuse lipid layer and the bulk water at a bilayer. (●) Anions; (○) cations.

and a neutral lipid L^0 (DPPC) to form a charged lipid complex, LA^- (8,17,18,36,42,43,92–98): $L^0 + A^- \rightleftharpoons LA^-$. The binding constant K_A of the above reaction is defined as:

$$K_A = \frac{[LA^-]}{[L^0][A^-]_s} = \frac{x_b}{(1 - x_b)C_{A,\infty} \exp(q_e \phi_0 / k_B T)}, \quad (21)$$

where x_b is the percentage of lipid molecules that have acquired a charge through anion binding, $C_{A,\infty}$ is the concentration of ion A in the reference solution in (mol m^{-3}), and ϕ_0 is the electrostatic potential at the binding plane that is created due to anion adsorption on the lipid headgroups.

The surface charge density σ is given by the Grahame equation (53–55):

$$\sigma = \sqrt{8\mathfrak{R}T C_{A,\infty} \epsilon_0 \epsilon} \sinh\left(\frac{q_e \phi_0}{2k_B T}\right) = -\frac{q_e x_b}{a_L}. \quad (22)$$

Here the minus sign reflects the negative charge that builds at the lipid surface upon anion adsorption. Equations 21 and 22 constitute the basis of a charge regulation model often used in calculations in colloid and biophysical chemistry (99–101). For an assumed value of K_A the system of Eqs. 21 and 22 can be used to generate x_b , ϕ_0 , and σ . The nonlinear Poisson-Boltzmann equation is solved between the two bilayers with the boundary conditions: $(\frac{d\phi}{dx})_{x=0} = -\frac{\sigma}{\epsilon_0 \epsilon}$, and $(\frac{d\phi}{dx})_{x=d_w/2} = 0$. When the complete potential profile $\phi(x)$ is calculated, the electrostatic contribution to the osmotic pressure is obtained using Eq. 14, whereas the electrostatic free energy needed in Eq. 15 (in $\text{J (mol lipid)}^{-1}$) is given by the expression ((34); E. Leontidis, L. Belloni, and A. Aroti, unpublished data):

$$\Delta F_{\text{ele}} = -2x_b \mathfrak{R}T \tanh\left(\frac{q_e \phi_0}{4k_B T}\right) + \mathfrak{R}T \ln(1 - x_b). \quad (23)$$

The binding model can be generalized to treat the case of independent sodium ion adsorption on the lipid headgroups, although this can be expected to be weak, since the experimental result of Aroti et al. (1) was that the osmotic pressure curves in the presence of NaCl and NaBr are almost identical to those obtained in the absence of electrolytes. Previous attempts to fit phospholipid bilayer osmotic pressure have consistently avoided treating sodium adsorption (23,92–98). Recent computer simulation studies of DPPC bilayers in the presence of NaCl have revealed that sodium interacts with the lipids more strongly than chloride (102–110). In fact, the simulations suggest that sodium interacts with the carbonyl groups of the lipids with a complexation mechanism, each sodium ion coordinated by one to four different lipid molecules (103,106,108). Given this evidence it appears reasonable to examine the case of separate sodium binding. We will however assume that sodium binds to the lipids less strongly than the large chaotropic anions (NO_3^- , I^- , SCN^-), a notion supported by the experimental finding that the effect of NaI and NaSCN on the headgroup area and the interbilayer distance is very pronounced, whereas that of NaCl or NaBr is almost undetectable. In this case two binding constants are needed:

$$K_A = \frac{[LA^-]}{[L^0][A^-]} = \frac{x_{b,A}}{(1 - x_{b,A} - x_{b,Na^+})C_{A,\infty} \exp(q_e \phi_0 / k_B T)} \quad (24)$$

$$K_{Na^+} = \frac{[LNa^+]}{[L^0][Na^+]} = \frac{x_{b,Na^+}}{(1 - x_{b,A} - x_{b,Na^+})C_{Na,\infty} \exp(-q_e \phi_0 / k_B T)}, \quad (25)$$

and Eq. 22 becomes

$$\sigma = \sqrt{8\mathfrak{R}TC_{A,\infty}\varepsilon_0\varepsilon} \sinh\left(\frac{q_e\varphi_0}{2k_B T}\right) = -\frac{q_e(x_{b,A} - x_{b,Na^+})}{\alpha_L}, \quad (26)$$

whereas the electrostatic free energy is given by:

$$\Delta F_{\text{ele}} = -2(x_{b,A} - x_{b,Na^+})\mathfrak{R}T \tanh\left(\frac{q_e\varphi_0}{4k_B T}\right) + \mathfrak{R}T \ln(1 - x_{b,A} - x_{b,Na^+}). \quad (27)$$

The possibility of the simultaneous binding of an anion and a sodium ion on the same lipid molecule was not examined in this work.

Model of anion partitioning in a diffuse lipid layer

This model is based on the concept of an active diffuse interface (33,34), as shown in Fig. 1 *b* for two approaching bilayers. In this model, the interface (water-lipid) is divided in two regions. For $x \geq \delta$ the classical nonlinear Poisson-Boltzmann equation (PBE) applies, the analytical solution of which for 1:1 electrolytes is as follows (53–55):

$$\tanh\left(\frac{q_e\varphi(x)}{4k_B T}\right) = \tanh\left(\frac{q_e\varphi_\delta}{4k_B T}\right) e^{-\kappa(x-\delta)}, \quad (28)$$

where φ_δ is the electrostatic potential at $x = \delta$ and κ is the Debye length of the reference solution. The top region ($0 \leq x < \delta$), of thickness δ , is playing an active role in the process of ion adsorption and is responsible for the ionic “selectivity” of the interface with respect to the bulk ($\delta < x \leq d_w/2$). Ion partitioning is driven by an attractive chemical potential U_i , which is constant for each ionic species i . For $0 \leq x < \delta$ the PBE is transformed into the following equation for a 1:1 electrolyte, assuming the dielectric constant is equal to that of bulk water:

$$\frac{d^2\varphi}{dx^2} = -\frac{q_e C_\infty}{\varepsilon_0\varepsilon} \left(e^{-(q_e\varphi + U_+)/k_B T} + e^{+(q_e\varphi - U_-)/k_B T} \right). \quad (29)$$

By setting $U_+ \rightarrow \infty$ for $0 \leq x < \delta$ we exclude the cations from the lipid layer. The resulting equation has then an analytical solution, which is as follows for monovalent anions ((34,111); E. Leontidis, L. Belloni, and A. Aroti, unpublished data):

$$C_-(x) = \frac{C_0}{\cos^2\left(\frac{Yx}{\delta}\right)}, \quad (30)$$

where Y is a dimensionless parameter defined as

$$Y = \sqrt{2\pi L_B N_{AV} C_0 \delta^2}. \quad (31)$$

C_0 is the anion concentration at $x = 0$, given by:

$$C_0 = C_\infty \exp\left(\frac{q_e\varphi_0 - U_-}{k_B T}\right), \quad (32)$$

and L_B is the Bjerrum length

$$L_B = \frac{q_e^2}{4\pi\varepsilon\varepsilon_0 k_B T}. \quad (33)$$

At $x = \delta$ the electrostatic potentials and electric fields ($E = -\nabla\varphi$) calculated in the two regions must match. The following two conditions can then be derived:

$$q_e\phi_\delta = U_- + k_B T \ln\left(\frac{C_0}{C_\infty \cos^2 Y}\right) \quad (34)$$

$$Y \tan Y = -\kappa \delta \sinh\left(\frac{q_e\varphi_\delta}{2k_B T}\right). \quad (35)$$

For a given U_- using a combination of Eqs. 31, 34, and 35 one can compute φ_δ , C_0 , and Y , and then the complete electrostatic potential profile in the region between two bilayers. The electrostatic contribution to the total osmotic pressure exerted between the lipid bilayers is calculated using Eq. 14 as before. The electrostatic potential ϕ_{med} at the midplane can be calculated from Eq. 28, once ϕ_δ is known. Finally, the electrostatic contribution to the free energy per mol lipid in the context of this model is as follows ((34); E. Leontidis, L. Belloni, and A. Aroti, unpublished data):

$$\Delta F_{\text{ele}} = -2x_b \mathfrak{R}T \tanh\left(\frac{q_e\varphi_\delta}{4k_B T}\right) + \frac{Y a_L \mathfrak{R}T}{2\pi L_B \delta} (2 \tan Y - Y). \quad (36)$$

Equations 23 and 36 differ only in the second term of the right-hand side, since the first term is the contribution of the diffuse double layer. Sodium partitioning in the diffuse lipid layer can be treated quite easily in this model, but the solution of Eq. 29 must then be found numerically. The osmotic pressure is obtained again from Eq. 14, with properly computed values of the midplane potential, ϕ_{med} . The electrostatic free energy per mol of lipid is obtained numerically from the integral:

$$\Delta F_{\text{ele}} = \mathfrak{R}T \int \left\{ \frac{1}{2} \varepsilon \varepsilon_0 (\nabla\varphi)^2 + C_\infty \left[-\left(1 + \frac{q_e\varphi}{k_B T}\right) \exp\left(-\frac{q_e\varphi + U_+}{k_B T}\right) + \left(-1 + \frac{q_e\varphi}{k_B T}\right) \exp\left(\frac{q_e\varphi - U_-}{k_B T}\right) \right] + 2\Theta(x - \delta) \right\} dx, \quad (37)$$

where Θ is a Heavyside step function (E. Leontidis, L. Belloni, and A. Aroti, unpublished data).

Fitting the osmotic pressure isotherms: discussion

Fitting the DPPC/Water isotherm

The detailed fitting analysis required to reduce the parameters of the perpendicular EOS to an absolute minimum starts from the fit of the $\log\Pi-d_w$ in the absence of electrolytes, hence in the absence of the electrostatic repulsion. This allows the comparison with older literature results (6,51, 59,112). The computed fitting parameters are then adjusted in the case of salts, the electrostatic force added, and the binding or partitioning parameters generated. To fit the experimental $\log\Pi-d_w$ curves one must take into consideration the four parameters P_0 , λ , κ_c , and H in Eqs. 10, 11 or 12, and 13. In principle one should use the full model equations containing all the adjustable parameters and carry out a non-linear regression procedure to simultaneously fit all parameters to the data. However, this would only be feasible if a large number of experimental points were available. We have therefore chosen a different fitting process, which is described in more detail in Appendix I. Several alternative sets of parameters can be used to fit the $\log\Pi-d_w$ experimental results for DPPC bilayers in pure water equally well. Assuming the power-law expression (Eq. 11) for the undulation force, and for values of the Hamaker constant, H , in the range of 0.8–1.2 $k_B T$, one can find reasonable (according to the literature) values for the bending rigidity, which provide excellent fits to the data. In general, it was found that excellent fits were obtained for $H = (1.0 \pm 0.2) k_B T$, $\lambda = (2.55 \pm 0.05) \text{ \AA}$, $P_0 = (8.67 \pm 0.06) \times 10^8 \text{ Pa}$ and a wide range of κ_c values (from 9 to 30 $k_B T$). Similarly, if one uses the exponential expression of Eq. 12 for the undulation force, one can find reasonable values for the bending rigidity and get excellent fits to the data. In Supplementary Fig. S1, *a* and *b*, in Supplementary Material we present the best fitting curves for DPPC in water for the two different fluctuation force expressions.

Comparing the results found here and those reported in Table 1 by other researchers we notice that the present parameters do not agree closely with those found by other research

groups in the past (6,51,59,112). This may be due to the fact that Lis et al. (112) and Rand et al. (6) calculated the hydration coefficient, P_0 , and hydration length, λ , without taking into account the maximum swelling point. McIntosh et al. (51) used an additional exponential steric repulsive force to fit the force curve of DPPC in pure water. McIntosh et al. (51) and Petrache et al. (59) used a different way to define the water bilayer separation (using the electron density profile of the bilayers), and in addition they used the exponential form of the fluctuation force. Thus significant differences can be expected between the parameters reported and those from this work, although the results of Petrache et al. (59) are in fair agreement with the results obtained by us with the exponential fluctuation force. In conclusion, it can be said that the values found for the different parameters over the years are strongly model-dependent, and as a result no perfect agreement can be found.

Fitting the DPPC/electrolyte isotherms using the binding model

The experimental $\log\Pi-d_w$ curves for DPPC in the presence of salt solutions of different concentrations are fitted according to the following procedure: All the parameters that have been obtained (P_0 , λ , and κ_c) using the conditional fitting for DPPC in water (as explained before) are kept unchanged. P_0 and λ should not change since the experimental data at all salt concentrations and for all salt types converge at high Π , in agreement with previous observations in the literature (8); κ_c should decrease slightly in the presence of salt solutions (30) but the decrease is expected to be small ($\sim k_B T$) compared to the values actually used in this work, and thus is not taken into account. The Hamaker constant should decrease by $\sim 50\%$ according to existing theory (28,29), and in agreement with the recent work by Petrache et al. (23), who found a gradual decrease of the Hamaker constant for neutral PC multilamellar vesicles with KBr or KCl concentration to values $< 50\%$ of that in the absence of salt. A binding constant K_A (M^{-1}) for the anions is introduced that determines the electrostatic repulsive force generated between the lipid bilayers due to anion adsorption. Different values for the binding constant are used until the best fit to the experimental results is found. The results

TABLE 1 Parameter values from several fits to $\log\Pi-d_w$ force curves for DPPC in water at 50°C

DPPC/Water parameters	Lis et al. (112)*	Rand et al. (6)		McIntosh et al. (51)	Petrache et al. (59)			Aroti et al. (this work) [†]	
H (kT)	0.75	—	—	0.70	1.16	0.70	1.80	1.0 ± 0.2	1.8 ± 0.2
P_0 (Pa)	$10^{9.99}$	$10^{9.38}$ g	10^{10} c	$10^{7.6}$	10^8	$10^{7.96}$	$10^{7.76}$	10^9	$10^{9.4}$
λ (Å)	2.2	2.55 g	2.13 c	1.38	1.97	1.97	2.39	2.55 ± 0.05	2.10 ± 0.1
κ_c (kT)	—	—	—	25	12	24	24	9 to 30	35 ± 2
K (dyne/cm ²)	—	—	145	—	—	—	—	—	—

*Values taken from the literature cited in the table.

[†]Values were obtained in this work using a power-law (left column) and an exponential expression (right column) for the undulation force. g, gravimetric method; c, compressibility method.

reported below have all been obtained with the power-law form of the fluctuation force. The behavior observed with the exponential fluctuation force was similar, with some differences in the numerical values of the various parameters, and will not be discussed further.

In a first round of calculations we have neglected sodium binding on the DPPC headgroups, as has been done in the past by most researchers in the field (23,92–98), and have based our calculations on Eqs. 21–23. As a general observation, the $\log\Pi-d_w$ curves (including the maximum swelling point) of DPPC in the presence of low salt concentrations (0.05 and 0.1 M) using the binding model, cannot be fitted at all, unless the Hamaker constant is allowed to increase very substantially. Even thus, for a 0.5-M salt concentration a very large binding constant must be used to fit the experimental $\log\Pi-d_w$ data. It would appear that an additional repulsive force is required to fit the experimental results for DPPC both in NaSCN and NaI salt solutions of concentration 0.5 M (see Supplementary Figs. S2 and S3 in Supplementary Material). To improve the fit and reduce the binding constant to values comparable to those found for the lower NaSCN and NaI concentrations we must assume a physically unrealistic Stern layer for Na^+ adsorption (4–8 Å) (results not shown). This is not an acceptable solution, since the Pauling radius for Na^+ is only 1 Å (80–82). Stern layers are more meaningful at rigid interfaces and not at this fluid interface at 50°C. The fact that the Hamaker constant must increase so much raises serious doubts about the fitting process, because theoretically the low frequency part of the Hamaker constant must decrease in the presence of a salt solution by a factor proportional to $\exp(-2\kappa d_w)$, where κ^{-1} is the Debye length of the solution (23,28,29,54). At high salt concentration, as the water refractive index approaching that of the lipids (34,113), even the high frequency contribution to the Hamaker constant may decrease, as demonstrated by Petrache et al. (23). We thus anticipate that the Hamaker constant will be reduced by at least 50% when salts are present. It is therefore necessary to question the assumption that the osmotic pressure goes to zero at the maximum swelling point. The presence of minute amounts of impurities could increase the osmotic pressure at the maximum swelling point to a value of 100–200 Pa, which is extremely hard to detect and measure precisely. There exists also the possibility of equilibrium of the swollen bilayers with a system of vesicles under tension (114,115). During any multilayered vesicle formation process, the outer layers in onion-like structures are under lateral stress. As a result, at “osmotic equilibrium” the compression due to tensile stresses of the outer layers dominate the residual osmotic pressure, which may be of the order of 100–200 Pa, as was discussed by Diamant et al. (116). A less likely possibility, given the extremely low solubility of DPPC (117), is the salting-in of lipids by the chaotropic salts, which might increase their solubility in solution. Other possible arguments in favor of a nonzero osmotic pressure at maximum swelling will be discussed later.

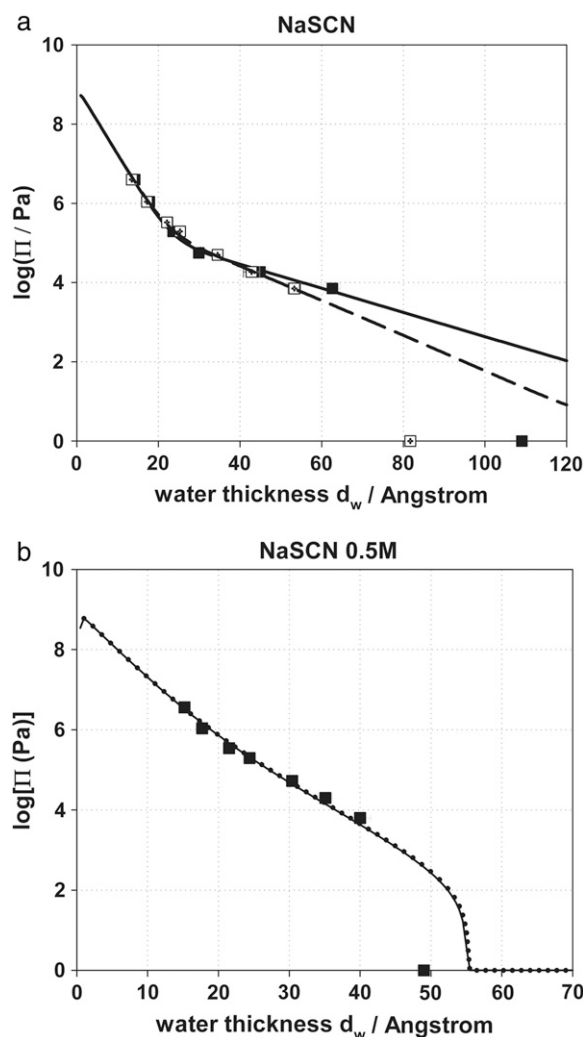


FIGURE 2 (a) Fitting curves obtained from the binding model for DPPC in the presence of 0.05 M (■) and 0.1 M (□) NaSCN (excluding the maximum swelling point). Hamaker constant = $0.4 k_B T$. $K_A = 3.5 \text{ M}^{-1}$ and $K_A = 4.0 \text{ M}^{-1}$ for NaSCN concentration 0.05 and 0.1 M, respectively. (b) Fitting curves obtained from the binding model for DPPC in the presence of 0.5 M NaSCN (excluding the maximum swelling point). Hamaker constant = $0.4 k_B T$. $K_A = 200 \text{ M}^{-1}$ (solid line) and $K_A = 300 \text{ M}^{-1}$ (dotted line).

As a result, we decided to fit the experimental $\log\Pi-d_w$ results without taking into account the maximum swelling point. A value half of that found for DPPC in water ($H = 0.4 k_B T$) was assumed for the Hamaker constant. Fig. 2, a and b, show the best fitting curves found for DPPC in the presence of NaSCN of various concentrations using the binding model. Similar fitting curves are obtained for DPPC in the presence of NaI, NaNO_3 , and NaBr. Table 2 shows the best binding constants for each salt concentration obtained without the maximum swelling point. The results in Fig. 2 and Table 2 imply that an ever increasing binding constant must be assumed as electrolyte concentration increases to provide good fits to the data. The increase of K_A at 0.5 M NaSCN is excessive, corresponding to complete surface saturation

TABLE 2 Fitted binding constants of anions A^- on the headgroups of DPPC molecules for different concentrations of NaA salt solutions

Concentration/M	Binding constants			
	K_{Br}/M^{-1}	K_{NO_3}/M^{-1}	K_I/M^{-1}	K_{SCN}/M^{-1}
0.05	—	—	0.9 ± 0.1	3.5 ± 0.1
0.1	0.2 ± 0.1	0.4 ± 0.1	1.6 ± 0.1	4.0 ± 0.1
0.5	>0.4	>0.8	>100	>200

with ions. The binding constants reported in Table 2 are clearly not thermodynamic quantities, and only indicate qualitatively that the salts examined here follow the Hofmeister series. An additional attempt to fit the NaSCN data at 0.5 M was made by setting K_A equal to $3.5 M^{-1}$ (the value found at 0.05 M) and allowing the Hamaker constant to gradually decrease. The curves in Fig. 3 show that even setting the Hamaker constant equal to zero in the high salt case will not lead to consistency between the low salt and high salt data.

Finally, we have repeated the calculations assuming that sodium binds to the lipids as well and using Eqs. 24–27 for the electrostatics. Fig. 4 and Table 3 summarize the findings, which were very similar to those in the absence of sodium binding. It is possible to find several pairs of sodium and anion binding constants that produce good fits to the osmotic pressure curves at low electrolyte concentrations, although even then a slight tendency for larger binding constants is observed at 0.1 M. When the concentration increases to 0.5 M it is no more possible to fit the data in a reasonable way, excessive values of the anion binding constant being needed. We therefore conclude that sodium binding will not explain the high salt results for NaI or NaSCN.

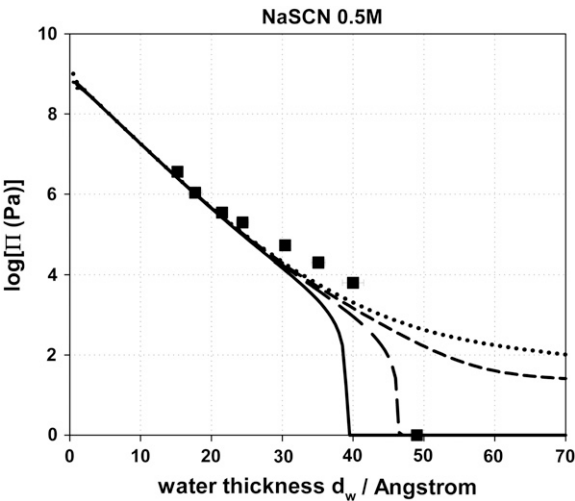


FIGURE 3 Fitting curves obtained from the binding model for DPPC in the presence of 0.5 M NaSCN, setting $K_A = 3.5 M^{-1}$ and allowing the Hamaker constant to decrease and eventually drop to zero. The values for H are $0.8 k_B T$ (solid line), $0.4 k_B T$ (long-dashed line), $0.2 k_B T$ (short-dashed line), and zero (dotted line).

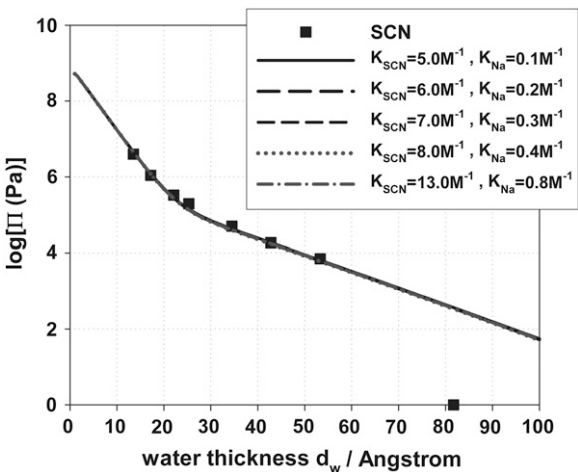


FIGURE 4 Fitting curves obtained from the binding model for DPPC in the presence of 0.1 M NaSCN with different binding constants for sodium (excluding the maximum swelling point). Hamaker constant = $0.4 k_B T$.

Fitting the DPPC/electrolyte isotherms using the diffuse lipid layer model

The previous calculations might be viewed as proof that the local anion binding model does not work in the DPPC bilayers. We have therefore carried out fitting calculations using the model of ionic partitioning into the lipid layer. A fitting procedure similar to that for the binding model was used (maximum swelling was not taken into account). The thickness of the diffuse lipid layer was set equal to $\delta = 4 \text{ \AA}$, which is roughly the average headgroup size of a DPPC molecule, excluding the glycerol group (6,10,118), but values as large as 10 \AA have also been examined. The lipid layer thickness was kept fixed ($\delta = 4 \text{ \AA}$) for all concentrations of all salts to avoid the introduction of an additional adjustable parameter. Calculations using different values of δ provide comparable fits to the data with different values of U_i (see Eq. 38 below). The fitting curves are very similar to those

TABLE 3 Fitted binding constants of anions I^- and SCN^- on the headgroups of DPPC molecules for different concentrations of NaA salt solutions taking into account the binding of Na^+ ions

Binding constants					
Salt concentration = 0.05 M					
K_{Na}/M^{-1}	0.1	0.2	0.3	0.4	0.8
K_I/M^{-1}	1.2	1.5	1.8	2.1	3.3
K_{SCN}/M^{-1}	4.5	5.5	6.5	7.5	11.5
Salt concentration = 0.1 M					
K_{Na}/M^{-1}	0.1	0.2	0.3	0.4	0.8
K_I/M^{-1}	1.9	2.3	2.8	3.3	5.3
K_{SCN}/M^{-1}	5.0	6.0	7.0	8.0	13.0
Salt concentration = 0.5 M					
K_{Na}/M^{-1}	0.1	0.2	0.3	0.4	0.8
K_I/M^{-1}			No fit		
K_{SCN}/M^{-1}					

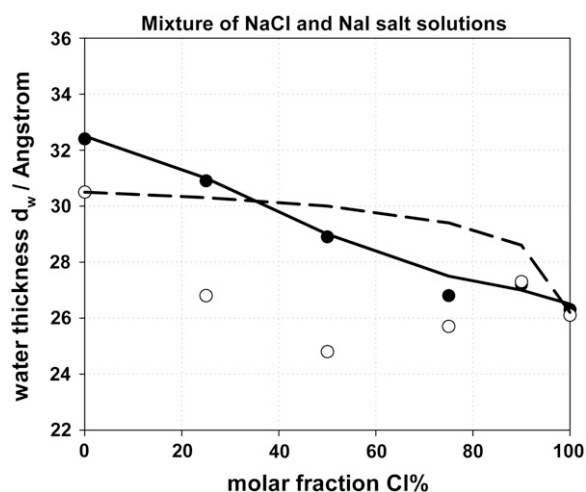


FIGURE 5 Fitting attempts with the binding model for the interbilayer water thickness of DPPC in mixtures of NaCl and NaI salt solutions at concentrations 0.1 and 0.5 M. A power-law-fluctuation force and no sodium binding is assumed. The osmotic pressure in all these experiments was set equal to $\log\Pi = 4.6$. Total $[NaCl] + [NaI] = 0.1$ M (●) and $[NaCl] + [NaI] = 0.5$ M (○).

observed using the binding model, as shown in Fig. 5 for DPPC in the presence of 0.05, 0.1, and 0.5 M NaSCN solutions. Similar results were also obtained for NaI. The interaction potentials U_- of the anions, obtained from these fits are summarized in Table 4. These interaction potentials depend on the anion used, but also on the concentration of the electrolyte solution. The binding constants and interaction potentials increase following the Hofmeister series of anions $Br^- < NO_3^- < I^- < SCN^-$ for the same salt concentration; for different salt concentrations the interaction potentials increase with concentration. Generally, the binding constants of anions estimated using the binding model demonstrate the same behavior as the interaction potentials, U_- . In fact, the binding constants of anions obtained from the binding model can be roughly transformed to interaction potentials using the following approximate expression. This approximate expression is derived by combining the charge regulation expression, Eq. 21, with the U_- viewed as a partitioning parameter: $[A^-]_{LL}/[A^-]_s = \exp(-\beta U_-)$, where $[A^-]_{LL}$ is the mean concentration of ion A^- within the lipid layer ($[A^-]_{LL} = [LA^-]/\delta$ to use the terminology of Eq. 21).

$$a_L \delta N_A v e^{-\frac{U_A}{k_B T}} \approx K_A. \quad (38)$$

TABLE 4 Fitted interaction potentials of anions A^- with the DPPC headgroup layer for different concentrations of NaA salt solutions

Concentration/M	0.05 M	0.1 M	0.5 M
Salts	$U_-/k_B T$	$U_-/k_B T$	$U_-/k_B T$
NaBr	—	−0.3	−0.9
NaNO ₃	—	−0.9	−1.6
NaI	−1.7	−2.3	−6.3
NaSCN	−3.1	−3.2	−7.0

TABLE 5 Fitted interaction potentials of the SCN^- ion with the DPPC headgroup layer for different concentrations of NaA salt solutions taking into account the partitioning of Na^+ ions in that layer

		Partitioning constants						
		Salt concentration = 0.05 M						
$U_{Na}/k_B T$	2.52	1.52	0.52	−0.12	−0.52	−1.52	−2.52	
$U_{SCN}/k_B T$	−3.00	−3.05	−3.25	−3.50	−3.65	−4.25	−4.85	
Salt concentration = 0.1 M								
$U_{Na}/k_B T$	2.52	1.52	0.52	−0.12	−0.52	−1.52	−2.52	
$U_{SCN}/k_B T$	−3.25	−3.30	−3.50	−3.70	−3.90	−4.50	−5.30	
Salt concentration = 0.5 M								
$U_{Na}/k_B T$	2.52	1.52	0.52	0.12	−0.12	−0.52	−1.52	−2.52
$U_{SCN}/k_B T$					No fit			

The partitioning model has also been extended by assuming that sodium partitions in the lipid layers as well. The results are summarized in Table 5 and a plot of fitting curves is provided in the Supplementary Material (Supplementary Fig. S4). Once more it can be seen that introducing a stronger sodium-lipid interaction does not allow fitting the osmotic pressure results over the entire salt concentration range. The problem observed at 0.5 M is thus a genuine effect, which illustrates that some important aspect is missing from the modeling platform adopted here. The problem is apparently not connected to the way that the electrostatic boundary condition at the lipid surfaces is handled.

Fitting the ion competition experiments using the binding model

The results of the ion-competition experiment described in the first article of this series were fitted as follows. Briefly, all the parameters that have been obtained (P_0 , λ , and κ_c) using the conditional fitting for DPPC in pure water (no sodium binding, power-law fluctuation force) were kept unchanged. The Hamaker constant was taken equal to $H = 0.4 k_B T$, a value half of that found for DPPC in pure water. The electrostatic contribution to the osmotic pressure was calculated taking into account a single binding constant value for the chloride anion and a single K_A for the iodide anion at a total salt concentration $[NaCl] + [NaI] = 0.1$ or 0.5 M, respectively. The binding constants of individual ions were calculated by considering the limiting cases of single electrolyte systems. The binding constant of chloride on DPPC was calculated from the data for pure NaCl as salt, by fitting the value of the water bilayer separation d_w at a total osmotic pressure $\log\Pi$ equal to 4.6 Pa. Similarly, the binding constant of iodide on DPPC was obtained from the data for pure NaI. The calculated binding constants were then used to fit the experimental results obtained when both NaI and NaCl are present at fixed total $[NaCl] + [NaI]$ concentration. The

fitting attempts are shown in Fig. 5 for total $[NaCl] + [NaI] = 0.1$ and 0.5 M. At 0.1 M the experimental results are fitted quite well using the binding constants obtained for the pure electrolyte systems, in agreement with the recent results of Petrache et al. (23), who carried out similar competition experiments for the KBr/KCl pair. At 0.5 M total salt concentration, however, d_w is no more a linear function of the salt concentration ratio, and the binding model performs quite poorly. The surprising minimum observed experimentally is not reproduced by the model. This result further demonstrates that there is a missing element in the models, which plays an important role at high concentrations of adsorbing salts.

Fitting the lateral EOS: discussion

We have verified that the combination of Eqs. 17, 18, and 20 can reproduce the equilibrium area per molecule for DPPC bilayers in the absence of salts (~ 70 Å² per molecule). However, it is not clear how to reproduce the dehydration-induced decrease of the area per molecule in the presence of nonpenetrating electrolytes. In addition, the model free energy minimum is rather deep, so that when the electrostatic free energy is added it is not possible to shift it in a measurable way in the presence of a strongly binding salt. Fig. 6 summarizes model predictions for bilayers in pure H₂O and 0.1 M and 0.5 M NaSCN and juxtaposes them to the

experimental results of the previous article (1). The electrostatic free energy was calculated with the partitioning model, but the choice of electrostatic model does not make a difference at all. We have used the interaction parameter $U_{SCN} = -3.2$ k_BT, which was found satisfactory for the perpendicular EOS and for 0.05 M and 0.1 M NaSCN. If we use Eqs. 17, 18, and 20 without any corrections and add the electrostatic free energy, we see that the model does not predict any strong change of the area per molecule in contrast to experiment. Modifying a_0 to $a_0 + x_b \Delta a_i$ in Eq. 17 does not make a difference as well, but if we also make the same modification in Eq. 18 then we obtain a measurable increase of the predicted areas. Exactly the same behavior is observed when Eq. 19 is used for the headgroup repulsions instead of Eq. 18. A final “improvement” is obtained if the conformational free energy of Eq. 20 is “softened,” i.e., reduced, by a factor of 2. The increase of the predicted area with salt concentration is then considerable. However, it still appears impossible to predict the maximum found experimentally at 0.1 M, which demonstrates that all these empirical lateral free energy terms are missing some important aspect of the salt-lipid interactions. The most surprising finding of this exercise is that the purely electrostatic free energy may not be the real reason for the lateral expansion of the bilayer surface. The modification of headgroup interactions and the softening of the conformational free energy of the tails in the presence of adsorbing salt appear to be responsible for the large effect of the salt on the lipid molecular area.

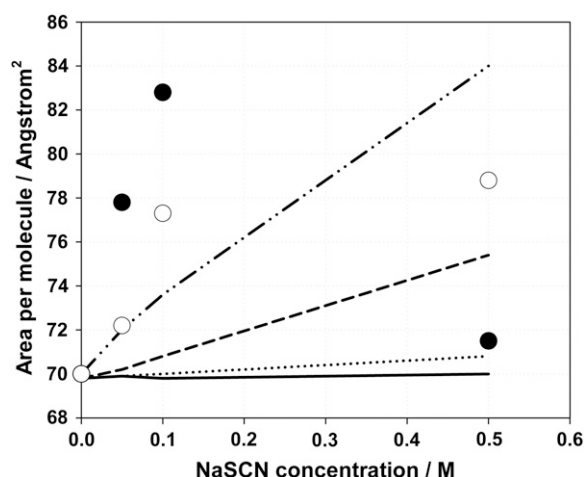


FIGURE 6 Fitting attempts for the lateral EOS. The headgroup areas of DPPC molecules in bilayers for pure water and for 0.1 M and 0.5 M NaSCN solutions are compared to model predictions. The total osmotic pressure was equal to $\log \Pi = 4.20$ – 4.30 in all cases. The solid curve is the combination of Eqs. 17, 18, and 20, without modification of a_0 . The dotted curve is the same combination with a_0 modified for anion adsorption only for Eq. 17. The dashed curve is the same combination of equations with a_0 modified for anion adsorption for both Eqs. 17 and 18. The dashed-dotted curve is the result of the combination of Eqs. 17, 19, and 20, with a_0 modified in Eqs. 17 and 19, and the terms in Eq. 20 diminished by 50%. The symbols are the experimental results of Aroti et al. (1) (●, NaSCN; ○, NaI).

Returning to the perpendicular EOS to explain the high-salt discrepancy

A case for solution nonideality

Our theoretical tools were not found adequate when the salt concentration became higher than 0.1 M. This is rather unfortunate, since salt concentrations higher than 0.1 M are typically encountered in many biological samples. What is the origin of this discrepancy? One possible answer is that solution nonidealities may be the answer to the fitting problems encountered. The fact that two rather different models for the treatment of the ion-lipid interaction provide very similar results is an indication that the treatment of the diffuse double layer may be at fault. Returning to Eq. 14 we observe that the osmotic pressure is calculated both at the midplane and in the reference solution using the ideal Van't Hoff's law. This is not quite correct. For 0.5 M NaSCN solutions we know for example that the osmotic coefficients between 0.1 and 0.7 M are in the range of 0.93 – 0.95 (120). Working with a local thermodynamic approach the group of Sanfeld and Defay provided 40 years ago a more general expression of the electrostatic contribution to the osmotic pressure between two lipid surfaces in the presence of a fully dissociating 1:1 electrolyte (121):

$$\Pi_{\text{ele}} = \frac{k_B T C_\infty \left[\nu_{\text{med}} \frac{\gamma_{+, \infty}}{\gamma_{+, \text{med}}} e^{-q_e \phi_{\text{med}} / k_B T} + \nu_{\text{med}} \frac{\gamma_{-, \infty}}{\gamma_{-, \text{med}}} e^{q_e \phi_{\text{med}} / k_B T} - 2\nu_\infty \right]}{1 + \nu_{\text{med}} C_\infty \left[\frac{\gamma_{+, \infty}}{\gamma_{+, \text{med}}} \nu_+ e^{-q_e \phi_{\text{med}} / k_B T} + \frac{\gamma_{-, \infty}}{\gamma_{-, \text{med}}} \nu_- e^{q_e \phi_{\text{med}} / k_B T} \right]} \quad (39)$$

In Eq. 39, ν_{med} and ν_∞ are the osmotic coefficients at the midplane and in the reference solution, respectively, $\gamma_{i, \text{med}}$ and $\gamma_{i, \infty}$ are the corresponding single ion activity coefficients, and ν_i are the ionic specific molar volumes. An order of magnitude analysis shows that the term involving square brackets in the denominator of Eq. 39 is of order 10^{-2} and can be ignored. Equation 14 can be derived from Eq. 39 if we set the activity coefficient ratios and the osmotic coefficients equal to unity. Apparently this is not a good approximation at high ionic strengths. In Fig. 7 we plot Π_{ele} as a function of d_w for a 0.5 M NaSCN solution, as calculated from Eq. 39, assuming: a), that the activity coefficient ratios are equal to one and $\nu_m = \nu_\infty = 1.0$ (case equivalent to Eq. 14); b), that the activity coefficient ratios are equal to one and $\nu_m = \nu_\infty = 0.943$; and c), that the activity coefficient ratios are equal to one and $\nu_m = 0.944$, $\nu_\infty = 0.943$. It can be seen that a difference of 0.001 between the osmotic coefficients of the midplane and the reference solution is indeed capable of reproducing the increased repulsion observed in the perpendicular EOS, and even of partly explaining the fact that the osmotic pressure does not go to zero at maximum swelling conditions. This is of course only a rough calculation, since at large values of d_w the two osmotic coefficients should

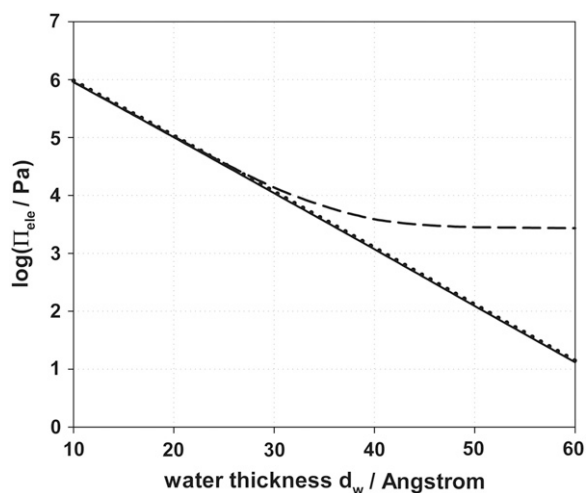


FIGURE 7 Electrostatic osmotic pressure as a function of bilayer separation using the ideal Van t' Hoff law (*dashed curve*), Eq. 39 without the activity coefficients and setting the osmotic coefficients (*a*) both equal to unity (*solid curve*), (*b*) both equal to the literature value of 0.943 for bulk 0.5 M NaSCN (*dotted curve*), and (*c*) setting the midplane osmotic coefficient to 0.944 and the bulk osmotic coefficient to 0.943 (*dash-dotted curve*).

eventually become identical, but it shows that analyzing perpendicular EOS data from bilayer experiments requires better bulk information for the electrolyte solutions. More advanced theory is also needed. There is no currently acceptable equation that provides single-ion activity coefficients and solution osmotic coefficients within double layers, in a situation where local electroneutrality does not hold. Improved double layer models invariably start from statistical mechanical approaches and are based on more complete ion-pair distribution functions, sometimes involving ionic hydration (82,90,91). Simple predictive equations of general acceptance have not been developed to date however.

A case for ion-lipid headgroup interactions

The detailed analysis of the lateral EOS revealed that the adsorption of chaotropic ions may modify intrabilayer free energy terms and in particular the headgroup repulsions and the conformational free energy of the lipid tails. Could this modification have an impact on the osmotic pressure as well? This would only be the case if the “surface” terms were also affected by the interbilayer distance d_w . Take for example the free energy term of Eq. 17 in the presence of ionic adsorption, where a_0 has been replaced by $a_0 + x_b \Delta a_i$. Differentiation of this term in the spirit of Eq. 7, would provide an osmotic pressure contribution:

$$\Pi_{\text{st}} = \gamma \frac{\Delta a_i}{a_L} \left(\frac{\partial x_b}{\partial d_w} \right)_{a_L, T, n_L} \quad (40)$$

Similarly, the headgroup interaction term of Eq. 18 would provide an osmotic pressure contribution:

$$\Pi_{\text{hg}} = -k_B T \frac{\Delta a_i}{a_L (a_L - a_0 - x_b \Delta a_i)} \left(\frac{\partial x_b}{\partial d_w} \right)_{a_L, T, n_L} \quad (41)$$

This raises the serious possibility that intrabilayer terms can affect the osmotic pressure through the derivative of x_b with d_w . From the basic theory of double-layer interaction (53–55) we know that the osmotic pressure of two parallel flat plates decays exponentially with d_w because it is roughly proportional to ϕ_{med}^2 . Would the derivative in Eqs. 40 and 41 behave in the same way? We have calculated x_b for the case of 0.5 M NaSCN as a function of d_w from the partitioning model as the integral of anions found in the 4-Å-thick lipid layer, where anions partition, divided by the total number of lipid molecules:

$$x_b = \frac{A_{\text{tot}} \int_0^\delta N_{\text{AV}} C_{\text{SCN}} dx}{n_L} = a_L N_{\text{AV}} \int_0^\delta C_{\text{SCN}} dx \quad (42)$$

We have also numerically computed the derivative $(\partial x_b / \partial d_w)$ for this case using experimental for a range of experimental d_w values. Finally we have computed the median electrical potential in the context of this model. In Fig. 8 we plot the derivative $(\partial x_b / \partial d_w)$ as a function of ϕ_{med}^2 and

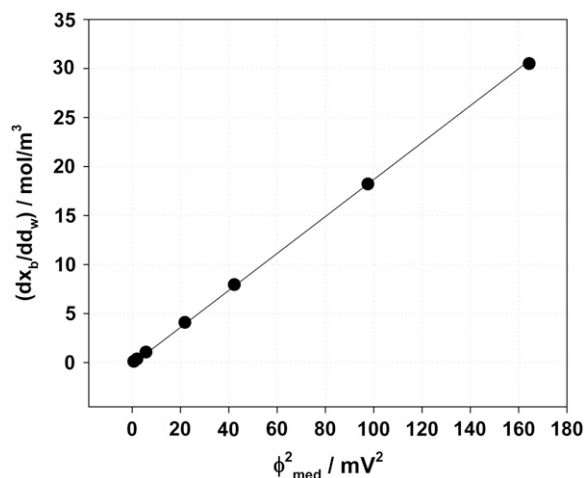


FIGURE 8 Plot of the derivative $(\partial x_b / \partial d_w)$ as a function of ϕ_{med}^2 for the case of 0.5 M NaSCN. Both quantities were calculated using the ion-partitioning model, an interfacial layer thickness of 4 Å, and an interaction parameter of $-3.2 \text{ k}_B\text{T}$ for NaSCN.

observe a remarkable linearity. This is a clear indication that any surface free energy term that is affected by the degree of anion binding may provide “well-behaved” osmotic pressure terms that may add up at high salt and low osmotic pressures to provide the apparent additional repulsion observed experimentally. An order of magnitude analysis with Eqs. 40 and 41 shows that the expected pressures range from hundreds to thousands of Pa! Because the lateral EOS analysis leaves much to be desired we have not pursued this point further.

CONCLUSIONS

Perpendicular equation-of-state (osmotic pressure) data for bilayers of DPPC in the presence of various salts can be fitted reasonably well at low salt concentrations using either a local binding or an interfacial partitioning model for the ionic electrostatic contribution to the osmotic pressure. A slight discrepancy can, however, be detected between 0.05 and 0.1 M, larger binding parameters being necessary for the higher concentrations. The ion-lipid binding or partitioning constants follow the Hofmeister series as expected. Single-salt binding constants can be used to fit the results of an ion competition experiment between iodide and chloride, in which the separation of the bilayers was measured at a specific osmotic pressure, keeping the total NaI+NaCl concentration constant and varying the ratio of iodide to chloride in the system.

The results are different at 0.5 M salt. Binding and partitioning models fail to reproduce the perpendicular EOS with the same parameters as for small salt concentrations; in fact, unnaturally large binding parameters are needed to fit the data. This difficulty is observed irrespectively of whether the maximum swelling point is taken into account or not. A

similar behavior is observed in the ion competition experiments. The binding constants of Cl^- and I^- obtained at 0.1 M cannot fit the experimental results for a total NaI+NaCl concentration equal to 0.5 M. Several explanations for this failure of current theory may be put forward. It is possible that in the presence of very high concentrations of chaotropic ions the interface is considerably “softened” and the perpendicular headgroup fluctuations (protrusion forces) (50) increase considerably. Another possibility is that the interfacial rigidity increases, leading to stronger undulation repulsion, although this is in contrast to theoretical considerations and is not visible as increased peak broadening of the small-angle x-ray scattering (SAXS) peaks for DPPC in the presence of NaSCN (34). In fact, the SAXS peaks appear to become thinner (less broad) as the electrolyte concentration increases (results not shown). Petrache et al. (122) have also observed that even at very high salt concentrations the membrane rigidity (bending rigidity) was not altered, implying that the repulsive fluctuation force does not change in the presence of salts.

Modeling approaches similar to ours have been used extensively in the past to fit perpendicular EOS for lipid bilayers in the presence of salts (8). Fitting was always found problematic at large concentrations. The recent work by Petrache et al. (23) is a considerable step forward, after many years in which real progress was not made, since they proved that a careful modeling of the effect of electrolytes on the Hamaker constant of the bilayers allows an almost quantitative modeling of the perpendicular EOS at salt concentrations up to 0.1 M. However, this work demonstrates that all problems have not been solved, especially at higher salt concentrations and more strongly adsorbing ions.

The lateral EOS was also examined in this work to provide additional information about the ion-lipid interaction. This is one of very few examples (22,24,123) where a combined fitting of the lateral and perpendicular phospholipids EOS in the presence of electrolytes is attempted. Our simple free energy approach for the lateral EOS relied on information obtained from fitting the perpendicular EOS. The results are not very encouraging. A reasonable compatibility appears to exist between the lateral and the perpendicular EOS, with the same binding constant probably satisfactory in both cases. The lateral EOS calculations proved however that the present phenomenological models are not satisfactory, since they do not provide information on how to treat the case of strongly adsorbing ions. We see indications that the adsorbed ions may affect headgroup interactions and even tail conformational entropy. Currently no existing theory can describe in a consistent way the effect of adsorbed ions on the lipid headgroup conformation and interactions. Simple approaches such as that of Mbamala et al. (27) or elaborations of more complex models, such as that of Stigter and Dill (74–76) may provide insights in the near future. The very few existing results from computer simulations of bilayers in the presence of electrolytes other than NaCl suggest that large anions

penetrate deeply into the lipid headgroup layer and may affect the headgroup orientation and interactions (110).

Regarding the difficulty of explaining the osmotic pressure results at high concentration of adsorbing salts, we have put forward two tentative explanations in this work. On the one hand we have argued that this discrepancy may have its origin in the incomplete modeling of the diffuse double layer, which does not incorporate ion hydration, activity, and osmotic coefficient effects. On the other hand we have found evidence that intrabilayer free energy terms depending on the “degree of binding” may contribute to the osmotic pressure of the bilayers in ways compatible with what is observed experimentally. This work highlights our relative ignorance about ion-lipid interaction at interfaces, and points out the need for more extensive experiments and better theory in this area.

The definite answer about the mechanism of action of the Hofmeister series in these soft lipid interfaces can be approached, if unique association constants of the ions with the lipids are deduced from experiment. Only then it will become possible to correlate these constants with ionic properties or ion-lipid and ion-water interactions and make real progress toward the solution of this long-standing riddle.

APPENDIX I

To fit the experimental $\log\Pi-d_w$ curves, for a specific value of the Hamaker constant, H , the hydration decay length, λ , was set and the hydration coefficient, P_0 , was varied over a broad range of values. For each H , λ , and P_0 , we calculate the model deviation from the experimental points as a sum of pointwise square deviations. The best value of P_0 (for each λ) is considered to be that which leads to the smallest error. The procedure is facilitated considerably by the fact that there are known limits in the values that the different parameters can take. For example, the Hamaker constant has been estimated to vary between 0.25 and 2.5 $k_B T$ (6,51,54,124), the bending rigidity usually ranges between 10 and 50 $k_B T$ (125,126) for fluid bilayers, the hydration coefficient ranges between $10^{7.5}$ and 10^{10} Pa (5–7,51), and the hydration decay length is expected to vary between 1.8 and 2.6 Å (6,51,59,112). These values are more or less established by various studies on neutral and charged lipid bilayers that have been carried out in the past 20–30 years.

For a specific value of the Hamaker constant (e.g., $H = 1.0 k_B T$) the hydration decay length, λ , is varied usually from 1.8 to 2.8 Å. For each value of λ the error function is calculated for a total of 1000 different values of P_0 . The bending rigidity, κ_c , is evaluated each time by requiring that the fitting curve passes exactly from the maximum swelling point. The same theoretical analysis was followed for different values of the Hamaker constant. The results show that the hydration decay length, λ , and the hydration coefficient, P_0 , are not greatly influenced by the change of the Hamaker constant.

SUPPLEMENTARY MATERIAL

To view all of the supplemental files associated with this article, visit www.biophysj.org.

Financial support for this work was provided by the French-German Network, Commissariat de l'Énergie Atomique (CEA) Saclay, France, the Max Planck Institute of Colloids and Interfaces Golm/Potsdam, Germany, and research grants from the University of Cyprus.

REFERENCES

1. Aroti, A., E. Leontidis, M. Dubois, and T. Zemb. 2007. Effects of monovalent anions of the Hofmeister series on DPPC lipid bilayers. Part I. Swelling and in-plane equations of state. *Biophys. J.* 93:1580–1590.
2. Collins, K. D., and M. W. Washabaugh. 1985. The Hofmeister effect and the behaviour of water at interfaces. *Q. Rev. Biophys.* 18:323–422.
3. Cacace, M. G., E. M. Landau, and J. J. Ramsden. 1997. The Hofmeister series: salt and solvent effects on interfacial phenomena. *Q. Rev. Biophys.* 30:241–277.
4. Baldwin, R. L. 1996. How Hofmeister ion interactions affect protein stability. *Biophys. J.* 71:2056–2063.
5. Parsegian, V. A., R. P. Rand, N. L. Fuller, and D. C. Rau. 1986. Osmotic stress for the direct measurement of intermolecular forces. *Methods Enzymol.* 127:400–416.
6. Rand, R. P., and V. A. Parsegian. 1989. Hydration forces between phospholipid bilayers. *Bioch. Biophys. Acta.* 988:351–376.
7. Parsegian, V. A., and R. P. Rand. 1995. Interaction in membrane assemblies. In *Structure and Dynamics of Membranes*. R. Lipowsky and E. Sackmann, editors. Elsevier, Amsterdam, The Netherlands.
8. Lis, L. J., V. A. Parsegian, and R. P. Rand. 1981. Binding of divalent cations to dipalmitoylphosphatidylcholine bilayers and its effect on bilayer interaction. *Biochemistry.* 20:1761–1770.
9. Loosley-Millman, M. E., R. P. Rand, and V. A. Parsegian. 1982. Effects of monovalent ion binding and screening on measured electrostatic forces between charged phospholipid-bilayers. *Biophys. J.* 40:221–232.
10. McIntosh, T. J., and S. A. Simon. 1986. Hydration force and bilayer deformation: a reevaluation. *Biochemistry.* 25:4058–4066.
11. McIntosh, T. J., A. D. Magid, and S. A. Simon. 1989. Range of the solvation pressure between lipid membranes: dependence on the packing density of solvent molecules. *Biochemistry.* 28:7904–7912.
12. Afzal, S., W. J. Tesler, S. K. Blessing, J. M. Collins, and L. J. Lis. 1984. Hydration force between phosphatidylcholine surfaces in aqueous electrolyte solutions. *J. Colloid Int. Sci.* 97:303–307.
13. Cunningham, B. A., and L. J. Lis. 1989. Interactive forces between phosphatidylcholine bilayers in monovalent salt solutions. *J. Colloid Int. Sci.* 128:15–25.
14. Zemb, T., L. Belloni, M. Dubois, and S. Marcelja. 1992. Osmotic pressure of highly charged swollen bilayers. *Prog. Colloid Polym. Sci.* 89:33–38.
15. Demé, B., M. Dubois, and T. Zemb. 2002. Swelling of a lecithin lamellar phase induced by small carbohydrate solutes. *Biophys. J.* 82:215–225.
16. Lis, L. J., M. McAlister, N. Fuller, and R. P. Rand. 1982. Measurement of the lateral compressibility of several phospholipid bilayers. *Biophys. J.* 37:667–672.
17. Ohshima, H., and T. Mitsui. 1978. Theory of effects of calcium-ions on lamellar phase of dipalmitoyl lecithin. *J. Colloid Int. Sci.* 63:525–537.
18. Ohshima, H., Y. Inoko, and T. Mitsui. 1982. Hamaker constant and binding constants of Ca^{2+} and Mg^{2+} in dipalmitoyl phosphatidylcholine/water system. *J. Colloid Int. Sci.* 86:57–72.
19. Tatulian, S. A., V. I. Gordeliy, A. E. Sokolova, and A. G. Syrykh. 1991. A neutron diffraction study of the influence of ions on phospholipid membrane interactions. *Biochim. Biophys. Acta.* 1070:143–151.
20. Cantú, L., M. Corti, E. Del Favero, and A. Raudino. 2000. Tightly packed lipid lamellae with large conformational flexibility in the interfacial region may exhibit multiple periodicity in their repeat distance. A theoretical analysis and x-ray verification. *Langmuir.* 16:8903–8911.
21. Ruckenstein, E., and M. Manciu. 2001. On the stability of lyotropic lamellar liquid crystals and the thicknesses of their lamellae. *Langmuir.* 17:5464–5475.

22. Forsman, J. 2006. Ion adsorption and lamellar-lamellar transitions in charged bilayer systems. *Langmuir*. 22:2975–2978.
23. Petrache, H. I., T. Zemb, L. Belloni, and V. A. Parsegian. 2006. Salt screening and specific ion adsorption determine neutral-lipid membrane interactions. *Proc. Natl. Acad. Sci. USA*. 103:7982–7987.
24. Harries, D., R. Podgornik, V. A. Parsegian, E. Mar-Or, and D. Andelman. 2006. Ion induced lamellar-lamellar phase transition in charged surfactant systems. *J. Chem. Phys.* 124:224702.
25. Yuet, P. K., and D. Blankschtein. 1996. Molecular thermodynamic modeling of mixed cationic/anionic vesicles. *Langmuir*. 12:3802–3818.
26. Fattal, D. R., D. Andelman, and A. Ben-Shaul. 1995. The vesicle-micelle transition in mixed lipid-surfactant systems: a molecular model. *Langmuir*. 11:1154–1161.
27. Mbamala, E. C., A. Fahr, and S. May. 2006. Electrostatic model for mixed cationic-zwitterionic lipid bilayers. *Langmuir*. 22:5129–5136.
28. Mahanty, J., and B. W. Ninham. 1976. Dispersion Forces. Academic Press, New York.
29. Parsegian, V. A. 2005. Van der Waals Forces: A Handbook for Biologists, Chemists, Engineers, and Physicists. Cambridge University Press, Cambridge, UK.
30. Brotons, G., M. Dubois, L. Belloni, I. Grillo, T. Narayanan, and T. Zemb. 2005. The role of counterions on the elasticity of highly charged lamellar phases: a small-angle x-ray and neutron-scattering determination. *J. Chem. Phys.* 123:024704.
31. Tatulian, S. A. 1993. Phospholipid Handbook. G. Cevc, editor. Marcel Dekker, NY.
32. Cevc, G. 1990. Membrane electrostatics. *Biochim. Biophys. Acta*. 1031:311–382.
33. Zemb, T., L. Belloni, M. Dubois, A. Aroti, and E. Leontidis. 2004. Can we use area per surfactant as a quantitative test model of specific ion effects? *Curr. Opin. Colloid Int. Sci.* 9:74–80.
34. Aroti, A. 2005. Study of the effect of Hofmeister anions on monolayer, bilayer and micelle lipid model systems through experiments and theory. PhD thesis. University of Cyprus, Nicosia, Cyprus.
35. Levine, S., G. M. Bell, and B. A. Pethica. 1964. Counter-ion penetration in ionized monolayers at a dielectric interface. *J. Chem. Phys.* 40:2304–2309.
36. Iso, K., and T. Okada. 2000. Evaluation of electrostatic potential induced by anion-dominated partition into zwitterionic micelles and origin of selectivity in anion uptake. *Langmuir*. 16:9199–9204.
37. Aroti, A., E. Leontidis, E. Maltseva, and G. Brezesinski. 2004. Effect of Hofmeister anions on DPPC Langmuir monolayers at the air-water interface. *J. Phys. Chem. B*. 108:15238–15245.
38. Ben Shaul, A., and W. M. Gelbart. 1985. Theory of chain packing in amphiphilic aggregates. *Annu. Rev. Phys. Chem.* 36:179–211.
39. Heindl, A., and H.-H. Kohler. 1996. Rod formation of ionic surfactants: a thermodynamic model. *Langmuir*. 12:2464–2477.
40. Bauer, A., S. Woelki, and H.-H. Kohler. 2004. Rod formation of ionic surfactants. Electrostatic and conformational energies. *J. Phys. Chem. B*. 108:2028–2037.
41. Andreev, V. A., and A. I. Victorov. 2006. Molecular thermodynamics for micellar branching in solutions of ionic surfactants. *Langmuir*. 22:8298–8310.
42. Copeland, B. R., and H. C. Andersen. 1981. A theory for ion binding and phase equilibria in charged lipid membranes. I. Proton binding. *J. Chem. Phys.* 74:2536–2547.
43. Copeland, B. R., and H. C. Andersen. 1981. Theory for ion binding and phase equilibria in charged lipid membranes. II. Competitive and cooperative binding. *J. Chem. Phys.* 74:2548–2558.
44. Lis, L. J., M. McAlister, N. Fuller, R. P. Rand, and V. A. Parsegian. 1982. Interactions between neutral phospholipid bilayer membranes. *Biophys. J.* 37:657–665.
45. Parsegian, V. A., R. P. Rand, and N. L. Fuller. 1991. Direct osmotic-stress measurements of hydration and electrostatic double-layer forces between bilayers of double-chained ammonium acetate surfactants. *J. Phys. Chem.* 95:4777–4782.
46. Issue devoted to the discussion of hydration forces. 1985. *Chem. Scr.* 25:1–116.
47. Ninham, B. W. 1989. Hydration forces—real and imagined. *Chem. Scr.* 29A:15–21.
48. Belaya, M. L., M. V. Feigel'man, and V. G. Levadny. 1987. Structural forces as a result of nonlocal water polarizability. *Langmuir*. 3:648–654.
49. Leikin, S., and A. A. Kornyshev. 1990. Theory of hydration forces. Nonlocal electrostatic interaction of neutral surfaces. *J. Chem. Phys.* 92:6890–6898.
50. Israelachvili, J. N., and H. Wennerström. 1992. Entropic forces between amphiphilic surfaces in liquids. *J. Phys. Chem.* 96:520–531.
51. McIntosh, T. J., and S. A. Simon. 1993. Contributions of hydration and steric (entropic) pressures to the interactions between phosphatidylcholine bilayers: experiments with the subgel phase. *Biochemistry*. 32:8374–8384.
52. Trokhymchuk, A., D. Henderson, and D. T. Wasan. 1999. A molecular theory of the hydration force in an electrolyte solution. *J. Colloid Int. Sci.* 210:320–331.
53. Cevc, G., and D. Marsh. 1987. Phospholipid Bilayers. Physical Principles and Models. J. Wiley and Sons, New York.
54. Israelachvili, J. 1991. Intermolecular and Surface Forces, 2nd Ed. Academic Press, London, UK.
55. Evans, D. F., and H. Wennerström. 1999. The Colloidal Domain, 2nd Ed. VCH Publishers, New York.
56. LeNeveu, D. M., R. P. Rand, V. A. Parsegian, and D. Gingell. 1977. Measurement and modification of forces between lecithin bilayers. *Biophys. J.* 18:209–230.
57. Rand, R. P., N. Fuller, V. A. Parsegian, and D. C. Rau. 1988. Variation in hydration forces between neutral phospholipid bilayers: evidence for hydration attraction. *Biochemistry*. 27:7711–7722.
58. Simon, S. A., and T. J. McIntosh. 1989. Magnitude of the solvation pressure depends on dipole potential. *Proc. Natl. Acad. Sci. USA*. 86:9263–9267.
59. Petrache, H. I., N. Goulaiev, S. Nagle-Tristram, R. Zhang, R. M. Suter, and J. F. Nagle. 1998. Interbilayer interactions from high-resolution x-ray scattering. *Phys. Rev. E*. 57:7014–7024.
60. Nagle, J. F., and S. Tristram-Nagle. 2000. Structure of lipid bilayers. *Biochim. Biophys. Acta*. 1469:159–195.
61. Tristram-Nagle, S., H. I. Petrache, and J. F. Nagle. 1998. Structure and interactions of fully hydrated dioleoylphosphatidylcholine bilayers. *Biophys. J.* 75:917–925.
62. Cevc, G., B. Žekš, and R. Podgornik. 1981. The undulations of hydrated phospholipid multilayers may be due to water-mediated bilayer-bilayer interactions. *Chem. Phys. Lett.* 84:209–212.
63. Evans, E. A., and V. A. Parsegian. 1986. Thermal-mechanical fluctuations enhance repulsion between bimolecular layers. *Proc. Natl. Acad. Sci. USA*. 83:7132–7136.
64. Evans, E., and D. Needham. 1987. Physical properties of surfactant bilayer membranes: thermal transitions, elasticity, rigidity, cohesion, and colloidal interactions. *J. Phys. Chem.* 91:4219–4228.
65. Podgornik, R., and V. A. Parsegian. 1992. Thermal-mechanical fluctuations of fluid membranes in confined geometries: the case of soft confinement. *Langmuir*. 8:557–562.
66. Somette, D., and N. Ostrowsky. 1984. Repulsive steric interaction between membranes of finite size. *J. Phys. (Paris)*. 45:265–271.
67. Somette, D., and N. Ostrowsky. 1986. Importance of membrane fluidity on bilayer interactions. *J. Chem. Phys.* 84:4062–4067.
68. Ninham, B. W., and V. A. Parsegian. 1970. Van der Waals interactions in multilayer systems. *J. Chem. Phys.* 53:3398–3402.
69. Podgornik, R., R. H. French, and V. A. Parsegian. 2006. Nonadditivity in van der Waals interactions within multilayers. *J. Chem. Phys.* 124:044709.

70. Parsegian, V. A. 1966. Theory of liquid-crystal phase transitions in lipid + water systems. *Trans. Faraday Soc.* 62:848–860.
71. Jönsson, B., and H. Wennerström. 1981. Thermodynamics of ionic amphiphile-water systems. *J. Colloid Int. Sci.* 80:482–496.
72. Katz, Y. 1988. Surface tension in phospholipid bilayers. *J. Colloid Int. Sci.* 122:92–99.
73. Cantor, R. S., and K. A. Dill. 1986. Theory for the equation of state of phospholipid monolayers. *Langmuir*. 2:331–337.
74. Stigter, D., and K. E. Dill. 1986. Interactions in dilute monolayers of long-chain ions at the interface between n-heptane and aqueous salt solutions. *Langmuir*. 2:791–796.
75. Stigter, D., and K. E. Dill. 1988. Lateral interactions among phospholipid head groups at the heptane/water interface. *Langmuir*. 4: 200–209.
76. Stigter, D., J. Mingins, and K. E. Dill. 1992. Phospholipid interactions in model membrane systems. II. Theory. *Biophys. J.* 61:1616–1629.
77. Gruen, D. W. R. 1981. A model for the chains in amphiphilic aggregates. I. Comparison with a molecular dynamics simulation of a bilayer. *J. Phys. Chem.* 89:146–153.
78. Dill, K. A., J. Naghizadeh, and J. A. Marqusee. 1988. Chain molecules at high densities at interfaces. *Annu. Rev. Phys. Chem.* 39: 425–461.
79. Cantor, R. S. 1999. Lipid compositions and the lateral pressure profile in bilayers. *Biophys. J.* 76:2625–2639.
80. Conway, B. E. 1981. *Ionic Hydration in Chemistry and Biophysics*. Elsevier, Amsterdam, The Netherlands.
81. Marcus, Y. 1997. *Ion Properties*. Marcel Dekker, New York.
82. Barthel, J. M. G., H. Krienke, and W. Kunz. 1998. *Physical Chemistry of Electrolyte Solutions*. Springer Verlag, Darmstadt, Germany.
83. Schiby, D., and E. Ruckenstein. 1983. On the coupling between the double-layer and the solvent polarization-fields. *Chem. Phys. Lett.* 100:277–281.
84. Huang, H., M. Manciu, and E. Ruckenstein. 2003. The effect of surface dipoles and of the field generated by a polarization gradient on the repulsive force. *J. Colloid Int. Sci.* 263:156–161.
85. Manciu, M., and E. Ruckenstein. 2004. The polarization model for hydration/double layer interactions: the role of the electrolyte ions. *Adv. Colloid Int. Sci.* 112:109–128.
86. Wang, C. C., and L. J. Bruner. 1978. Dielectric saturation of aqueous boundary-layers adjacent to charged bilayer membranes. *J. Membr. Biol.* 38:311–331.
87. Gur, Y., I. Ravina, and A. J. Babchin. 1978. On the electrical double layer theory. I. A numerical method for solving a generalized Poisson-Boltzmann equation. *J. Colloid Int. Sci.* 64:326–332.
88. Basu, S., and M. M. Sharma. 1994. Effect of dielectric saturation on disjoining pressure in thin films of aqueous electrolytes. *J. Colloid Int. Sci.* 165:355–366.
89. Paunov, V. N., R. I. Dimova, P. A. Kralchevsky, G. Broze, and A. Mehreteab. 1996. The hydration repulsion between charged surfaces as an interplay of volume exclusion and dielectric saturation effects. *J. Colloid Int. Sci.* 182:239–248.
90. Kjellander, R., A. P. Lyubartsev, and S. Marcelja. 2001. McMillan-Mayer theory for solvent effects in inhomogeneous systems: calculation of interaction pressure in aqueous electrical double layers. *J. Chem. Phys.* 114:9565–9577.
91. Forsman, J. 2004. A simple correlation-corrected Poisson-Boltzmann theory. *J. Phys. Chem. B.* 108:9236–9245.
92. Tatulian, S. A. 1983. Effect of lipid phase transition on the binding of anions to dimyristoylphosphatidylcholine liposomes. *Biochim. Biophys. Acta.* 736:189–195.
93. Hauser, H., C. C. Hinckley, J. Krebs, B. A. Levine, and M. C. Phillips. 1977. The interaction of ions with phosphatidylcholine bilayers. *Biochim. Biophys. Acta.* 468:364–377.
94. Westman, J., and G. Eriksson. 1979. The interaction of various lanthanide ions and some anions with phosphatidylcholine vesicle membranes. A ³¹P NMR study of the surface potential effects. *Biochim. Biophys. Acta.* 557:62–78.
95. Akutsu, H., and J. Seelig. 1981. Interaction of metal ions with phosphatidylcholine bilayer membranes. *Biochemistry*. 20:7366–7373.
96. Altenbach, C., and J. Seelig. 1984. Calcium binding to phosphatidylcholine bilayers as studied by deuterium magnetic resonance. Evidence for the formation of a calcium complex with two phospholipid molecules. *Biochemistry*. 23:3913–3920.
97. McDonald, P. M., and J. Seelig. 1988. Anion binding to neutral and positively charged lipid membranes. *Biochemistry*. 27:6769–6775.
98. Rydall, J. R., and P. M. McDonald. 1992. Investigation of anion binding to neutral lipid membranes using deuterium NMR. *Biochemistry*. 31:1092–1099.
99. Ninham, B. W., and V. A. Parsegian. 1971. Electrostatic potential between surfaces bearing ionizable groups in ionic equilibrium with physiologic saline solution. *J. Theor. Biol.* 31:405–428.
100. Bloch, J. M., and W. B. Yun. 1990. Condensation of monovalent and divalent metal-ions on a Langmuir monolayer. *Phys. Rev. A.* 41:844–862.
101. Kallay, N., V. Tomisic, V. Hrust, R. Pieri, and A. Chittofrati. 2003. Association of counterions with micelles. *Colloids Surf. A.* 222:95–101.
102. Kaznessis, Y. N., S. Kim, and R. G. Larson. 2002. Simulations of zwitterionic and anionic phospholipid monolayers. *Biophys. J.* 82: 1731–1742.
103. Pandit, S. A., D. Bostick, and M. L. Berkowitz. 2003. Molecular dynamics simulation of a dipalmitoylphosphatidylcholine bilayer with NaCl. *Biophys. J.* 84:3743–3750.
104. Pandit, S. A., D. Bostick, and M. L. Berkowitz. 2003. Mixed bilayer containing dipalmitoylphosphatidylcholine and dipalmitoylphosphatidylserine: lipid complexation, ion binding, and electrostatics. *Biophys. J.* 85:3120–3131.
105. Berkowitz, M. L., D. L. Bostick, and S. Pandit. 2006. Aqueous solutions next to phospholipid membrane surfaces: insights from simulations. *Chem. Rev.* 106:1527–1539.
106. Böckmann, R. A., A. Hac, T. Heimburg, and H. Grubmüller. 2003. Effect of sodium chloride on a lipid bilayer. *Biophys. J.* 85:1647–1655.
107. Böckmann, R. A., and H. Grubmüller. 2004. Multistep binding of divalent cations to phospholipid bilayers: a molecular dynamics study. *Angew. Chem. Int. Ed. Engl.* 43:1021–1024.
108. Gurtovenko, A. 2005. Asymmetry of lipid bilayers induced by monovalent salt: atomistic molecular-dynamics study. *J. Chem. Phys.* 122:244902.
109. Gurtovenko, A. A., M. Miettinen, M. Karttunen, and I. Vattulainen. 2005. Effect of monovalent salt on cationic lipid membranes as revealed by molecular dynamics simulations. *J. Phys. Chem. B.* 109: 21126–21134.
110. Sachs, J. N., H. Nanda, H. I. Petrache, and T. B. Woolf. 2004. Changes in phosphatidylcholine headgroup tilt and water order induced by monovalent salts. Molecular dynamics simulations. *Biophys. J.* 86:3772–3782.
111. Engström, S., and H. Wennerström. 1978. Ion condensation on planar surfaces: solution of Poisson-Boltzmann equation for two parallel charged plates. *J. Phys. Chem.* 82:2711–2714.
112. Lis, L. J., M. McAlister, N. Fuller, R. P. Rand, and V. A. Parsegian. 1982. Interactions between neutral phospholipid bilayer membranes. *Biophys. J.* 37:657–665.
113. Rober, C. W., and J. A. Melvin. 1982. *CRC Handbook of Chemistry and Physics*, 63rd Ed. CRC Press, Boca Raton, Florida.
114. Seifert, U. 1995. Self-consistent theory of bound vesicles. *Phys. Rev. Lett.* 74:5060–5063.
115. Bar-Ziv, R., T. Frisch, and E. Moses. 1995. Entropic expulsion in vesicles. *Phys. Rev. Lett.* 75:3481–3484.
116. Diamant, H., and M. E. Cates. 2001. Swelling kinetics of the onion phase. *Eur. Phys. J. E.* 4:223–232.
117. Buboltz, J. T., and G. W. Feigenson. 2005. Phospholipid solubility determined by equilibrium distribution between surface and bulk phases. *Langmuir*. 21:6296–6301.

118. Nagle, J. F., and S. Tristram-Nagle. 2000. Structure of lipid bilayers. *Biochim. Biophys. Acta.* 1469:159–195.
119. Reference deleted in proof.
120. Robinson, R. A. 1940. The activity coefficients of sodium and potassium thiocyanate in aqueous solution at 25° from isopiestic vapor pressure measurements. *J. Am. Chem. Soc.* 62:3130–3131.
121. Sanfeld, A., C. Devillez, and P. Terlinck. 1970. A local thermodynamical approach of the repulsive energy between colloidal particles. *J. Colloid Int. Sci.* 32:33–40.
122. Petrache, H. I., S. Tristram-Nagle, D. Harries, N. Kucerka, J. F. Nagle, and V. A. Parsegian. 2006. Swelling of phospholipids by monovalent salt. *J. Lipid Res.* 47:302–309.
123. Dubois, M., T. Zemb, N. Fuller, R. P. Rand, and V. A. Parsegian. 1998. Equation of state of a charged bilayer system: measure of the entropy of the lamellar-lamellar transition in DDABr. *J. Chem. Phys.* 108:7855–7869.
124. Parsegian, V. A. 1993. Reconciliation of van der Waals force measurements between phosphatidylcholine bilayers in water and between bilayer-coated mica surfaces. *Langmuir.* 9:3625–3628.
125. Evans, E. A., and W. Rawicz. 1990. Entropy-driven tension and bending elasticity in condensed-fluid membranes. *Phys. Rev. Lett.* 64:2094–2097.
126. Kummrow, M., and W. Helfrich. 1991. Deformation of giant lipid vesicles by electric fields. *Phys. Rev. A.* 44:8356–8360.